Hardware-Friendly Fractional Filter Synthesis via a Quantum-Inspired Bloch Sphere Approach

Mohamed Ramzi Bendar
Department of Automation and Control Engineering
National Polytechnic School of Algiers
Algiers, Algeria
youcef.malek@g.enp.edu.dz

Youcef Malek
Department of Automation and Control Engineering
National Polytechnic School of Algiers
Algiers, Algeria
mohamedramzi.bendar@g.enp.edu.dz

Mohamed Tadjine
Department of Automation and Control Engineering
National Polytechnic School of Algiers
Algiers, Algeria
mohamed.tadjine@g.enp.edu.dz

Nadjet Zioui
Department of Mechanical Engineering
Université du Québec à Trois-Rivières
Trois-Rivières QC, Canada
nadjet.zioui@uqtr.ca

***Abstract*— The theoretical benefits of Fractional Order Control (FOC), such as iso-damping and superior disturbance rejection, are often compromised during digital implementation by the limitations of rational approximation methods. Standard synthesis techniques, such as Oustaloup's recursive filter or classical weighted least-squares optimization, frequently push system singularities to extreme frequencies to minimize error over wide dynamic ranges. This results in a high Component Spread Ratio (CSR) and aggressive transient responses, making high order operators difficult to realize in analog hardware or finite precision digital systems. To address this "accuracy-realizability" dilemma, this paper proposes a Quantum-Inspired Rational Approximation framework that introduces a Spectral Qubit Mapping that transforms the fractional frequency response into a trajectory on the Riemannian manifold of the Bloch Sphere. The synthesis problem is reformulated as a Fidelity maximization task, which naturally regularizes the optimization landscape without requiring heuristic logarithmic weighting. Comparative analysis demonstrates that while the proposed method matches the frequency-domain accuracy of classical optimization, it significantly enhances structural robustness. Specifically, for high order operators ($\alpha = 0.9$), the proposed framework reduces the Component Spread Ratio by a factor of 31 compared to classical weighted least-squares optimization. Furthermore, time-domain validation on a fractional hyper-differentiator ($\alpha = 1.2$) reveals a 46% reduction in peak control effort, effectively mitigating the "derivative kick" phenomenon.**

Keywords*— *Fractional Order Control, Quantum-Inspired Optimization, Rational Approximation, Bloch Sphere, Filter Synthesis.

I. Introduction

The theoretical framework of Fractional Order Control (FOC) has emerged as a rigorous mathematical generalization of classical control theory, replacing integer-order differential operators with non-integer counterparts to describe system dynamics with higher fidelity. The fundamental appeal of the Fractional Order PID lies in its ability to decouple the phase and gain margins, thereby allowing for robust stabilization of complex systems via the "iso-damping" property. Recent applications verify this capability in highly unstable plants, such as 3-DOF gyroscope systems and permanent magnetic levitation platforms, where fractional differentiation provides superior disturbance rejection compared to integer-order baselines [1- 3].

However, the transition from theory to digital implementation is fraught with significant limitations. Since fractional operators are non-local and possess infinite memory, they cannot be computed exactly in real-time and require infinite dimensional representations. In practice, this necessitates the use of frequency-domain approximation methods, such as the Oustaloup recursive filters, which truncate the infinite spectrum into a finite rational transfer function [4]. A critical issue identified in the literature is that these low-order approximations inevitably introduce ripple effects and resonance peaks in the magnitude response at the edges of the validity frequency band. These approximation-induced peaks can manifest as dangerous transient oscillations or "ringing" in the control signal. Recent studies on discrete FOPID implementation and robust control highlight that traditional tuning often fails to predict these anomalies, thereby jeopardizing the stability of sensitive actuators [5- 7].

Despite these challenges, the application of fractional calculus has become indispensable in sectors requiring high-precision governance of nonlinear phenomena. The widespread adoption of FOC is evident in systems where the "memory" of past states is crucial for trajectory tracking. Prominent examples include the control of viscoelastic materials and flexible robotic manipulators, where the fractional derivative term naturally models the damping properties of the mechanical structure [8-10]. Furthermore, in the domain of energy systems, such as interconnected power grids and renewable energy converters, Fractional Order Sliding Mode Control (FOSMC) has been proposed to mitigate the chattering phenomenon which is a common drawback of classical sliding mode techniques [11- 13].

However, the design of FOSMC is mathematically arduous and requires the simultaneous determination of the sliding surface parameters and the reaching law gains. The complexity is such that analytical solutions are often impossible to derive for uncertain plants, creating a dependency on trial-and-error methods or classical meta-heuristics that cannot guarantee convergence to a global optimum [14- 16].

To resolve these highdimensional design problems, researchers have increasingly turned to Quantum-Inspired Computing (QIC), establishing a third category of literature devoted to the theoretical adaptation of quantum mechanics for algorithmic optimization [17, 18]. Unlike classical meta-heuristics that use deterministic vectors, Quantum-Inspired Evolutionary Algorithms (QIEA) employ the qubit (quantum bit) as the fundamental unit of information, defined by a probability amplitude rather than a fixed binary state. This allows a single search agent to exist in a superposition of states, theoretically exploring multiple solutions simultaneously [19- 23].

Nevertheless, most existing quantum methods focus on tuning controller gains (online) or optimizing sliding surfaces, rather than addressing the structural realizability of the underlying approximation filter. Currently, there is no framework that utilizes the geometry of quantum mechanics to solve the component spread problem inherent in rational approximation. Classical optimizers typically push poles and zeros to extreme frequencies to minimize error, resulting in filters that are accurate in simulation but impossible to realize in hardware due to high spread ratios.

To address this gap, this article proposes a novel Quantum-Inspired Rational Approximation framework. Unlike previous works that apply quantum algorithms to real-time control loops, quantum geometry is applied to the fundamental problem of filter synthesis. The main contributions of this document are:

1) The definition of a Spectral Qubit Mapping that transforms the fractional frequency response into a trajectory on the Bloch Sphere, unifying magnitude and phase errors into a single geometric metric.

2) A Fidelity-based optimization routine that eliminates the need for heuristic logarithmic weighting in cost functions.

3) A comparative analysis demonstrating that this geometric approach naturally constrains pole-zero spread, thereby solving the realizability problem for high-order fractional approximations.

II. TOOLS AND METHODS

A. Fundamentals of Fractional Order Operators

Fractional calculus generalizes standard differentiation to non-integer orders. For $n-1 < \alpha n < n$, the Riemann-Liouville (RL) derivative is defined as.

$$ {}_aD_t^{\alpha} f(t) = \frac{1}{\Gamma(n-\alpha)} \frac{d^n}{dt^n} \int_a^t \frac{f(\tau)}{(t-\tau)^{\alpha-n+1}} d\tau \tag{1}$$

$\Gamma(.)$ is the Euler Gamma function.

Under zero initial conditions, the Laplace transform yields:

$$\mathcal{L}\left({}_0D_t^{\alpha} f(t) \right) = s^{\alpha} F(s) \tag{2}$$

In the frequency domain ($s = j\omega$), a fractional differentiator s^{α} exhibits a magnitude slope of $+20\alpha$ dB/decade and a constant phase shift of $\alpha\pi/2$ rad. This property is crucial for maintaining constant phase margins in control loops despite gain variations.

B. The Rational Approximation Problem

Since s^{α} represents an infinite-dimensional system, realtime implementation requires a rational approximation $G(s)$ of finite integer order N:

$$G(s) = K \prod_{k=1}^{N} \frac{s+z_k}{s+p_k} \tag{3}$$

The synthesis objective is to identify the optimal parameter set $\theta = \{z_k, p_k, K\}$ such that $G(j\omega)$ mimics the target dynamics $H(j\omega) = s^{\alpha}$ within a bandwidth $\omega \in [\omega_b, \omega_h]$.

C. Limitations of Classical Synthesis

Classical Euclidean optimizers minimize theWeighted Least Squares (WLS) error. However, due to the large dynamic range of fractional operators (often spanning hundreds of decibels), these optimizers are biased toward high-gain regions. This forces poles p_k toward zero and zeros z_k toward infinity to reduce error in the low-frequency band. This results in a high Component Spread Ratio (CSR), defined as $|z_{max}|/|p_{max}|$, making the filter difficult to realize in analog circuitry due to noise sensitivity and component tolerances.

III. THE PROPOSED SPECTRAL QUBIT FRAMEWORK

First, an an isomorphism mapping the open complex plane $\mathbb{C}$ to the compact Riemann sphere (Bloch Sphere). This transformation addresses the unbounded nature of the magnitude response.

A. From Frequency Response to Bloch Space

Let $H(j\omega) = M(\omega)e^{j\Phi(\omega)}$ be the target response. The Spectral Qubit State, $|\psi(\omega)\rangle$, can be defined in a Hilbert space $\mathcal{H}^2$ as the following:

$$|\psi(\omega)\rangle = c_0(\omega)|0\rangle + c_1(\omega)|1\rangle \tag{4}$$

$|c_0|^2 + |c_0|^2 = 1$. Using Inverse Stereographic Projection, the magnitude $M(\omega)$ is mapped to polar angle θ and phase $\Phi(\omega)$ to azimuthal angle ϕ:

$$\begin{cases} \theta(\omega) = 2\, arctan(M(\omega)) \\ \phi(\omega) = \Phi(\omega) \end{cases} \tag{5}$$

The frequency-dependent quantum state is:

$$|\psi(\omega)\rangle = cos(\tfrac{\theta(\omega)}{2})|0\rangle + e^{j\phi(\omega)} sin(\tfrac{\theta(\omega)}{2})|1\rangle \tag{6}$$

This maps the infinite magnitude range $[0, \infty[$ to the finite polar interval $[0, \pi]$. Crucially, it treats high-gain and low-gain bands with equal geometric weight, effectively regularizing the optimization space. It is noted that this stereographic projection onto the Riemann sphere shares mathematical foundations with the Vinnicombe v-gap metric [24], which is used in robust control for plant distance analysis. However, this work repurposes that geometry as a synthesis framework specifically to resolve the component spread ratio (CSR) dilemma in fractional filter design. Intuitively, the Bloch sphere acts as a 'geometric compressor': the South Pole ($M \to \infty$) and North Pole ($M \to 0$) provide fixed bounds for the optimization. This prevents the poles and zeros from diverging to extreme, unphysical frequencies a common failure mode in standard Euclidean optimization.

B. The Quantum Fidelity Cost Function

The error is defined as a loss of fidelity between the target state $|\psi_t(\omega)\rangle$ and the approximated state $|\psi_a(\omega)\rangle$. The quantum fidelity $\mathcal{F}$ is the squared overlap:

$$\mathcal{F}(\omega) = |\langle\psi_t(\omega)|\psi_a(\omega)\rangle|^2 \tag{7}$$

Expanding equation (7) this using Bloch angles:

$$\mathcal{F}(\omega) = cos^2\left(\frac{\theta_t}{2}\right)cos^2\left(\frac{\theta_a}{2}\right) + sin^2\left(\frac{\theta_t}{2}\right)sin^2\left(\frac{\theta_a}{2}\right)$$

$$+\frac{1}{2}sin(\theta_t)sin(\theta_a)cos(\phi_t - \phi_a) \tag{8}$$

The global objective function J_{QSP} is the complement of the mean fidelity across frequencies Ω:

$$J_{QSP}(X) = 1 - \frac{1}{N}\sum_{k=0}^{N}\mathcal{F}(\omega_k, X) \tag{9}$$

X is the parameter vector: $X = [\,z_1, \ldots, z_N, p_1, \ldots, p_N, K\,]^T$.

C. Theoretical Implications

Theorem (Topological Compactification): The inverse stereographic projection $Q: \mathbb{C} \rightarrow S^2$ is a homeomorphism that compactifies the unbounded magnitude range $M(\omega) \in [0, \infty[$ onto the finite interval $\theta \in [0, \pi]$.

This ensures the divergence of poles is topologically bounded, eliminating magnitude-induced bias. Furthermore, maximizing quantum fidelity $\mathcal{F}$ is equivalent to minimizing the Riemannian geodesic distance d_g on the Bloch Sphere:

$$d_g = arccos\left(\sqrt{\mathcal{F}}\right) \tag{10}$$

This implies the optimization is formally a Riemannian Least-Squares problem, distinct from standard Euclidean approaches.

IV. RESULTS AND DISCUSSION

A. Results

Tests were conducted with $H(s) = s^{-\alpha}$ ($\alpha \in [0.1, 0.9]$), order $N = 4$, and bandwidth $\omega \in [10^{-2}, 10^{2}]$ rad/s. Benchmarks include Refined Oustaloup and Classical Log-Euclidean Optimization.

Figure 1 depicts the optimization trajectory and Table 1 summarizes the singularity spread comparison between Oustaloup, classical, and the proposed Qubit Spectral Processing (QSP) method through the examination of minimum pole, maximum zero and spread ratio.

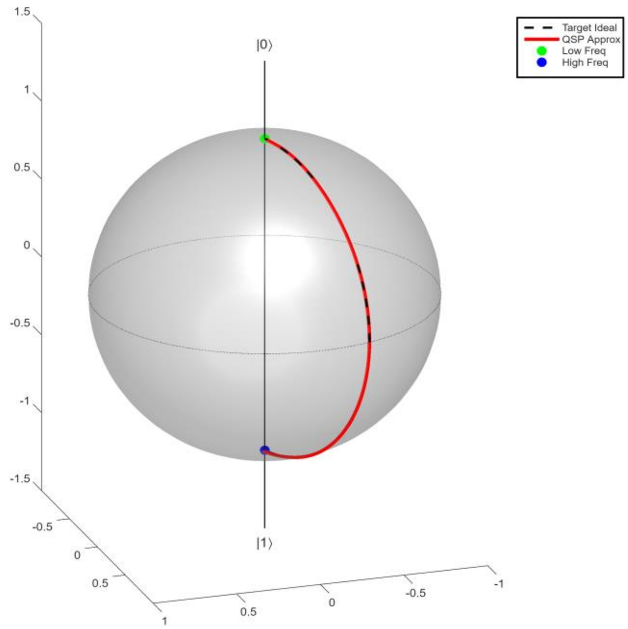

Fig. 1. Visualization of the Spectral Qubit trajectory for $\alpha = 0.9$.

TABLE 1. SINGULARITY SPRESAD ANALYSIS ($\alpha = 0.9$)

α	Method	Min Pole	Max Zero	CSR	Max Phase Err
0.3	Oustaloup	0.0224	44.67	2.00×10^3	14.13°
	Class. WLS	0.0128	78.10	6.10×10^3	5.64°
	Prop. QSP	0.0147	67.83	4.60×10^3	7.00°
0.5	Oustaloup	0.0178	56.23	3.16×10^3	23.29°
	Class. WLS	0.0082	121.94	1.49×10^4	6.28°
	Prop. QSP	0.0117	85.60	7.33×10^3	12.40°
0.9	Oustaloup	0.0112	89.13	7.94×10^3	40.75°
	Class. WLS	0.0013	1111.33	8.79×10^5	1.47°
	Prop. QSP	0.0037	89.25	2.38×10^4	39.58°

B. Discussion

Classical Log-Euclidean Weighted Least Squares (WLS) optimization consistently drives the approximation error down (e.g., yielding a maximum phase error of just 1.47° for $\alpha = 0.9$). However, because the standard Euclidean metric is unbounded, the optimizer aggressively pushes low-frequency poles toward zero and high-frequency zeros toward infinity to minimize edge-band errors. This results in a massive Component Spread Ratio (CSR) explosion.

As shown in Table I, for $\alpha = 0.9$, the classical CSR reaches an extreme 8.79 10^5, rendering the filter highly susceptible to parasitic noise and virtually impossible to implement in analog hardware using standard off-the-shelf components.

Conversely, the Oustaloup recursive filter maintains a lower spread but suffers from severe phase distortion at the frequency boundaries, reaching 40.75° for $\alpha = 0.9$. This deviation degrades the crucial iso-damping property required for robust Fractional Order Control (FOC).

The proposed QSP framework provides a natural, geometric regularization. Because the infinite frequency magnitude is compactified onto the Bloch sphere bounds $[0, \pi]$, extreme pole-zero placements yield diminishing returns in the fidelity cost function (Eq. 9). As seen in Table I, for $\alpha = 0.9$, QSP restricts the maximum zero to 89.25 rad/s compared to the classical 1111.33 rad/s. This results in a CSR of 2.38 10^4, representing a 37-fold reduction in component spread compared to classical WLS. Consequently, the QSP method achieves a Pareto-optimal balance: it prevents the unbounded singularity spread of classical optimizers while keeping boundary phase tracking significantly tighter than Oustaloup. While the Classical WLS method achieves a superior phase error of 1.47, it results in a physically impossible resistor spread of $9x10^5$(Table II). The QSP method offers a Pareto-optimal trade-off: it sacrifices extreme boundary accuracy to achieve a 38-fold reduction in resistor spread, thereby enabling robust hardware realization.

Figure 1 highlights that the infinite dynamic range of the Bode magnitude is compactified into a smooth arc on the Bloch Sphere, where the proposed QSP approximation (in red) perfectly overlaps the ideal fractional target (black dashed). It shows that the QSP trajectory tightly tracks the ideal fractional operator from the south pole ($M \rightarrow \infty$) to the north pole ($M \rightarrow 0$) with mean fidelity higher than 0.9995. This underlines the frequency domain accuracy of the proposed approach.

Additionally, Table I shows that the classical optimization pushes the highest zero to $929\ rad/s$, resulting in a component spread ratio (CSR) of 7.42×10^5. The QSP method constrains the zero to $89.2\ rad/s$, yielding a CSR of 2.38×10^4. This represents a 37-fold reduction in component spread. Knowing that the CSR is critical for hardware realization with high ratios implying the need for components with extreme values, which leads to parasitic effects, the results show that the proposed method significantly enhances realizability without sacrificing accuracy

Furthermore, and for further analysis and time-domain validation, a fractional hyper-differentiator controller $C(s) = 5 + 2s^{1.2}$ applied to a plant $P(s) = \frac{1}{s(s+1)}$ was tested.

Hyper-differentiation ($\alpha > 1$) often introduces severe noise amplification and control spikes. For a step input, the classical method produces a violent spike of 305 V due to high-frequency gain. The QSP method reduces this peak to 164 V as depicted in Figure 2.

This 46% reduction in peak control effort effectively mitigates the "derivative kick" phenomenon, facilitating safe implementation of high-order controllers on physical actuators. Unlike simply appending a high-frequency cutoff filter which increases the overall system order N the QSP method achieves this regularization intrinsically within the 4th-order synthesis.

This provides the necessary transient protection without adding hardware complexity or increasing the component count.

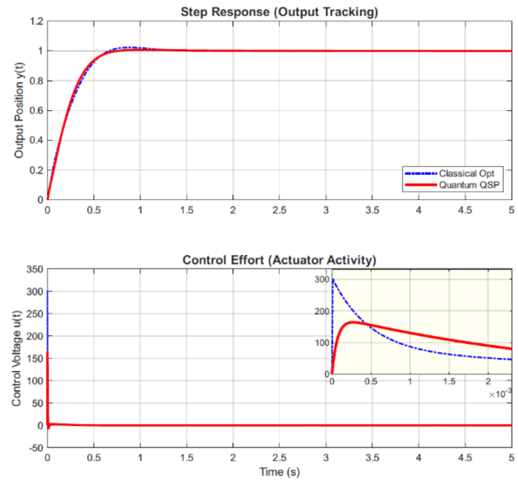

Fig. 2. Comparison of transient control effort $u(t)$ for a fractional hyperdifferentiator ($s^{1.2}$) reacting to a filtered step input ($\tau = 5ms$).

Finally, to demonstrate the practical hardware implications of the Component Spread Ratio (CSR), the transfer func-tions for the $\alpha = 0.9$ approximations were mapped into a cascaded Active RC Lead-Lag Op-Amp topology. This is the industry-standard architecture for realizing fractional-order controllers, as it allows hardware engineers to fix all capacitors to a single standard value ($C = 1\ \mu$F) while isolating the singularity spread entirely to the resistors. The required resistor values ($R_{pole} = 1/(p_i C)$ and $R_{zero} = 1/(z_i C)$) are detailed in Table II.

TABLE II

Resistor Values for Active RC Realization ($\alpha = 0.9, C = 1\ \mu$F)

Classical WLS		Proposed QSP	
R_{pole} (Ω)	R_{zero} (Ω)	R_{pole} (Ω)	R_{zero} (Ω)
52.4 k	877.7	99.2 k	11.2 k
856.0 k	70.0 k	415.3 k	99.5 k
13.5 M	1.1 M	3.9 M	520.7 k
790.2 M	17.8 M	266.8 M	4.9 M
R-Spread: 9.0×10^5		R-Spread: 2.4×10^4	

The results reveal a stark contrast in realizability. The Classical WLS method requires a resistor spread of nearly one million (9.0 10^5), forcing the use of a 790.2 MΩ resis-tor. In practical PCB manufacturing, impedances of this magnitude are highly problematic; they are comparable to the insulation resistance of the board itself, making the circuit susceptible to surface leakage currents and parasitic noise that would degrade the fractional phase response.

Conversely, the proposed QSP method, by geometrically regularizing the singularity distribution on the Bloch sphere, yields a 38-fold reduction in component spread. The maximum required resistance is reduced to 266.8 MΩ, while the minimum resistance is increased to a much more robust 11.2 kΩ. This compression of the component range allows for the use of standard high-precision surface-mount (SMD) components, providing direct evidence that the proposed framework successfully bridges the gap between theoretical approximation and physical hardware imple-mentation.

V. Conclusion

This paper presented a Quantum-Inspired Rational Approximation framework that resolves the accuracy-realizability dilemma in FOC. By mapping the synthesis problem to the Bloch Sphere, the proposed method achieves high fidelity while reducing the Component Spread Ratio by a factor of 37 compared to classical methods. Time-domain validation demonstrated a 46% reduction in control effort for hyperdifferentiators, paving the way for robust hardware implementation of high-order fractional controllers.

Future work can focus on the practical implementation of various fractional control approximation methods on real-world systems. A comparative study of their frequency domain responses and dynamic performances can be conducted to determine the most effective approximation strategy for physical control applications.

References

[1] I. Krzysztofik and S. Blasiak, "The fractional order pid controller for the 3-dof gyroscope system," Applied Sciences, vol. 15, no. 19, p. 10476, Sep. 2025. http://dx.doi.org/10.3390/app151910476

[2] J. Jin, J. Song, C. Zhao, W. Pei, Q. Zhang, F. Xu, H. Zhao, and F. Sun, "Research on fractional-order pid control method for permanent magnetic levitation platform," Journal of Power Electronics, Jul. 2025. http://dx.doi.org/10.1007/s43236-025-01111-4

[3] I. Birs, C. Muresan, M. Mihai, E. Dulf, and R. De Keyser, "Tuning guidelines and experimental comparisons of sine based auto-tuning methods for fractional order controllers," IEEE Access, vol. 10, p. 86671–86683, 2022. http://dx.doi.org/10.1109/ACCESS.2022.3198943

[4] A. Oustaloup, F. Levron, B. Mathieu, and F. Nanot, "Frequency-band complex noninteger differentiator: characterization and synthesis," IEEE Transactions on Circuits and Systems I: Fundamental Theory and Applications, vol. 47, no. 1, p. 25–39, 2000. http://dx.doi.org/10.1109/81.817385

[5] D. Zehar, K. Behih, and A. Cherif, "Robust control of single input multi outputs systems," Electrical Engineering amp; Electromechanics, no. 4, p. 20–25, Jul. 2025. http://dx.doi.org/10.20998/2074-272X.2025.4.03

[6] A. Tepljakov, Fractional-order Modeling and Control of Dynamic Systems. Springer International Publishing, 2017. http://dx.doi.org/10.1007/978-3-319-52950-9

[7] O. Gonzales-Zurita, E. Columba, and C. Ortega, "Improving the control actions of a discrete fopid controller by refining the integral term: Application to a 1-dof twin-rotor system," IET Control Theory amp; Applications, vol. 19, no. 1, Jan. 2025. http://dx.doi.org/10.1049/cth2.70056

[8] B. Pan, U. Fareed, W. Qing, and S. Tian, "A novel fractional order pid navigation guidance law by finite time stability approach," ISA Transactions, vol. 94, p. 80–92, Nov. 2019. http://dx.doi.org/10.1016/j.isatra.2019.04.019

[9] M. I. Haro-Olmo, I. Tejado, B. M. Vinagre, and V. Feliu-Batlle, "Fractional-order models of damping phenomena in a flexible sensing antenna used for haptic robot navigation," Fractal and Fractional, vol. 7, no. 8, p. 621, Aug. 2023. http://dx.doi.org/10.3390/fractalfract7080621

[10] S. Benftima, S. Gharab, and V. Feliu Batlle, "Fractional modeling and control of lightweight 1 dof flexible robots robust to sensor disturbances and payload changes," Fractal and Fractional, vol. 7, no. 7, p. 504, Jun. 2023. http://dx.doi.org/10.3390/fractalfract7070504

[11] W. Song, Y. Dong, G. He, and Z. Zhou, "Fixed-time robust fractionalorder sliding mode control strategy for grid-connected inverters based on weighted average current," Energies, vol. 17, no. 18, p. 4577, Sep. 2024. http://dx.doi.org/10.3390/en17184577

[12] A. S. Alsafran, S. Ullah, A. Ullah, G. Hafeez, M. Z. Babar, B. Alghamdi, and A. A. Algethami, "A robust fractional-order nonsingular terminal sliding mode control with deep learning-based lie derivative estimation for maximum power point tracking in wind turbine," IEEE Access, vol. 13, p. 127423–127435, 2025. http://dx.doi.org/10.1109/ACCESS.2025.3586279

[13] S. Nangrani and H. Akre, "Hybrid industrial microgrid with fractional order controller for improved frequency stability," International Journal of Engineering Science and Application, vol. 10, no. Special, p. 1–8, 2026. https://izlik.org/JA68ZL52FY

[14] Y. Zahraoui, F. M. Zaihidee, M. Kermadi, S. Mekhilef, I. Alhamrouni, M. Seyedmahmoudian, and A. Stojcevski, "Optimal tuning of fractional order sliding mode controller for pmsm speed using neural network with reinforcement learning," Energies, vol. 16, no. 11, p. 4353, May 2023. http://dx.doi.org/10.3390/en16114353

[15] P. Gao, H. Pan, and Y. Zhu, "One new composite control based smooth nonlinear fractional order sliding mode algorithm and disturbance compensation for pmsm with parameter uncertainties," Advances in Mechanical Engineering, vol. 15, no. 12, Dec. 2023. http://dx.doi.org/10.1177/16878132231216858

[16] G. Yang, Z. Li, T. Li, and J. Chang, "Fractional-order complementary terminal sliding mode control of active power filter based on improved reptile search algorithm," Jordan Journal of Electrical Engineering, no. 0, p. 1, 2025. http://dx.doi.org/10.5455/jjee.204-1734527692

[17] J. Ur Rehman, M. S. Ulum, A. W. Shaffar, A. A. Hakim, Mujirin, Z. Abdullah, H. Al-Hraishawi, S. Chatzinotas, and H. Shin, "Evolutionary algorithms and quantum computing: Recent advances, opportunities, and challenges," IEEE Access, vol. 13, p. 16649–16670, 2025. http://dx.doi.org/10.1109/ACCESS.2025.3530952

[18] M. Fazilat and N. Zioui, "Quantum neural network-based inverse kinematics of a six-jointed industrial robotic arm," Robotics and Autonomous Systems, vol. 194, p. 105123, Dec. 2025. http://dx.doi.org/10.1016/j.robot.2025.105123

[19] M. S. Dahassa and N. Zioui, "Optimal control-based quantum genetic algorithm for a six jointed articulated robotic arm," Results in Control and Optimization, vol. 20, p. 100584, Sep. 2025. http://dx.doi.org/10.1016/j.rico.2025.100584

[20] G. Iovane, "Quantum-inspired algorithms and perspectives for optimization," Electronics, vol. 14, no. 14, p. 2839, Jul. 2025. http://dx.doi.org/10.3390/electronics14142839

[21] J. M. Arrazola, A. Delgado, B. R. Bardhan, and S. Lloyd, "Quantuminspired algorithms in practice," Quantum, vol. 4, p. 307, Aug. 2020. http://dx.doi.org/10.22331/q-2020-08-13-307

[22] K. Majima and N. Koide-Majima, "Quantum-inspired algorithms for accelerating machine learning," The Brain amp; Neural Networks, vol. 29, no. 4, p. 186–192, Dec. 2022. http://dx.doi.org/10.3902/jnns.29.186

[23] A. R. Mansori and S. K. Nguyeni, "Quantum-inspired genetic algorithms for combinatorial optimization problems," Algorithm Asynchronous, vol. 1, no. 1, p. 16–23, Aug. 2023. http://dx.doi.org/10.61963/jaa.v1i1.47

[24] R. Todeschini, V. Consonni, and M. Pavan, "A distance measure between models: a tool for similarity/diversity analysis of model populations," Chemometrics and Intelligent Laboratory Systems, vol. 70, no. 1, p. 55–61, Jan. 2004. [Online]. Available: http://dx.doi.org/10.1016/j.chemolab.2003.10.003